Hindawi
Advances in Materials Science and Engineering
Volume 2019, Article ID 4382904, 10 pages
https://doi.org/10.1155/2019/4382904

*Research Article*

# Effect of Shear Creep on Long-Term Deformation Analysis of Long-Span Concrete Girder Bridge

**Yanwei Niu [1] and Yingying Tang [2]**

[1] *College of Highway, Chang'an University, Xi'an 710064, China*
[2] *College of Science, Chang'an University, Xi'an 710064, China*

Correspondence should be addressed to Yanwei Niu; niuyanwei@chd.edu.cn

Received 1 July 2019; Revised 23 October 2019; Accepted 22 November 2019; Published 13 December 2019

Academic Editor: Mohammad A. Hariri-Ardebili



The purpose of this paper is to report on the development of a three-dimensional (3D) creep calculation method suited for use in analyzing long-term deformation of long-span concrete girder bridges. Based on linear creep and the superposition principle, the proposed method can consider both shear creep and segmental multiage concrete effect, and a related program is developed. The effects of shear creep are introduced by applying this method to a continuous girder bridge with a main span of 100 m. Comparisons obtained with the nonshear case show that shear creep causes long-term deformation to increase by 12.5%. Furthermore, the effect of shear creep is proportional to the shear creep coefficient; for a bridge with different degrees of prestress, the influence of shear creep is close. Combined with the analysis of a continuous rigid bridge with a main span of 270 m, the results based on the general frame program suggest that shear creep amplification is multiplied by a factor of 1.13–1.15 in terms of long-term deformation. Moreover, the vertical prestress has little effect on shear creep and long-term deformation. The 3D creep analysis shows a larger long-term prestress loss for vertical prestress at a region near the pier cross section. The relevant computation method and result can be referenced for the design and long-term deformation analysis of similar bridges.

## 1. Introduction

Long-span concrete girder bridges (including continuous rigid-frame bridges) were first constructed in the 1950s. By utilizing the cantilever construction method, the difficulty of construction was greatly reduced, which caused this bridge type to develop rapidly. It gradually became the dominant bridge type in the medium- to large-span bridges. However, the problem of the excessive long-term deflection of long-span concrete bridges has frequently appeared in recent years [1–5] and has become a bottleneck restricting their development. Currently, the testing and computational effort involved in the problem of excessive long-term deformation is quite substantial and can mainly be divided into the following aspects: (1) long-term deflection observation and regular analysis of actual bridges [1–4]; (2) parameter analysis and suggestions for the control of long-term deflection [6–8]; and (3) improvement in long-term deflection calculation methods [9–15]. With regard to calculation methods, the current mainstream structure analysis software ignores the influence of shear creep. It is noted that an analysis of the long-span concrete girder bridge that ignores the effect of shear creep will cause error in the predicted value due to its large section and thin web [16]. In this regard, some scholars have proposed a more refined calculation method: Bažant et al. used a specialized material program based on ABAQUS to calculate the creep with a solid element model [11]. In addition, Cao et al. studied the effect of the law of cracks on the creep deformation of prestressed beams using experiments and proposed a relevant formula for analysis [12]. Moreover, Guo and Chen proposed a deflection control strategy for long-span concrete box-girder bridges based on field monitoring and probabilistic finite element (FE) analysis [13]. Niu et al. used ANSYS to develop a three-dimensional concrete creep calculation program [14]; Huang et al. developed a creep program based on ADINA to analyze the effect of shear lag [15]. Zhang et al. calculated the creep effect of reinforced concrete frames by fitting the axial creep curve [17]. However, the existing studies have not separated out the effects of shear creep. In this paper, for the long-span concrete girder bridge, a three-dimensional creep calculation method including segmental multiage concrete structures was considered and programmed by using MATLAB and ANSYS to realize a shear-creep-independent analysis. A continuous-girder bridge with a span of $65 + 100 + 65$ m was taken as an example of the analysis of the influence of shear creep on long-term deformation. The study examined the range of influence of shear creep on different prestressed bridges and the effect of vertical prestress on long-term deformation. The method of calculation of standard long-term deformation was discussed, and corresponding calculation suggestions were put forward.

## 2. Analysis Method

*2.1. Consideration of Shear Creep.* The long-term deformation analysis of concrete bridges can be divided into differential equations, algebraic equations, and a step-by-step approach [18]. It is generally accepted that the first two methods remain feasible for the analysis of simple structures. However, for complicated structures such as segmental multiage concrete bridges, the adoption of the step-by-step accumulation method based on the superposition principle is necessary, which is suitable for programming calculations. In this study, the step-by-step accumulation method is used to calculate the creep effect by changing the initial strain of each integration point of each concrete element. The formula for calculating the long-term strain of the integration point at time $t$ is as follows:

$$\varepsilon(t) = \frac{\sigma(t_0)}{E(t_0)}\left[1 + \phi(t, t_0)\right] + \sum_{i=1}^{n} \frac{\Delta\sigma(t_i)}{E(t_i)}\left[1 + \phi(t, t_i)\right] + \varepsilon_{cs}(t, t_0), \tag{1}$$

where $t$ is the calculation time (days), $t_0$ is the initial loading age of the concrete, $\sigma(t_0)$ is the initial stress, $E$ is the elastic modulus, and $\phi(t, t_0)$ is the creep coefficient. The first term of the formula represents the total strain generated by the initial stress, including elastic strain and creep strain. The age of concrete varies continuously from time $t_0$ to $t$, so the creep coefficient also varies. It must be divided into $n$ time steps to approximate this process. The creep coefficient of each time step is $\phi(t, t_i)$, and $\Delta\sigma(t_i)$ is the change in stress between the two adjacent times $t_i$ and $t_{i-1}$. $\varepsilon_{cs}(t, t_0)$ is the shrinkage strain, which can be calculated according to the standard formula [19]. Generally, in the planar frame FE creep computation, only three normal stresses (strains) are considered for each integration point. For three-dimensional (3D) solid or shell elements, the stress $\overline{\sigma}$ (and strain $\overline{\varepsilon}$) of the integration point is composed of six components as shown in the following equation:

$$\overline{\sigma} = \left\{\sigma_x, \sigma_y, \sigma_z, \tau_{xy}, \tau_{yz}, \tau_{xz}\right\}, \tag{2}$$

where $\sigma_x, \sigma_y, \sigma_z$ constitute the normal stress and $\tau_{xy}, \tau_{yz}, \tau_{xz}$ constitute the shear stress. The calculation of the influence on the shear deformation is achieved by using a 3D element and accounting for the creep effect of the shear stress. The creep correction coefficient is introduced to correct the creep coefficient of the six strain components $m\_\phi = [m_x, m_y, m_z, m_{xy}, m_{yz}, m_{xz}]$, where $m_x\,(\text{and}\, m_y, m_z) = 1$, and the axial creep is the same as the norm creep coefficient. On the contrary, if $m_{xy}\,(\text{and}\, m_{yz}, m_{xz}) = 1$, the shear creep coefficient is the same as that in the axial direction, and the modified shear value is calculated by a different shear creep coefficient. Specifically, if $m_{xy}$ (and $m_{yz}, m_{xz}$))is set to zero, the long-term deformation subjected to axial creep alone is calculated.

The creep deformation at any time $t_i$ is obtained by multiplying the elastic strain increment $\overline{\varepsilon}_0$, $(\overline{\varepsilon}_1 - \overline{\varepsilon}_0)$, $(\overline{\varepsilon}_2 - \overline{\varepsilon}_1), \ldots, (\overline{\varepsilon}_{i-1} - \overline{\varepsilon}_{i-2})$ of the previously calculated time point $t_0, t_1, \ldots, t_{i-1}$ by the creep coefficient $\phi(t_i, t_\tau)$ of the corresponding time, wherein $t_\tau$ is the age of loading. Under the action of a dead load, the stress of the statically determinate structure no longer changes. Therefore, except for the initial elastic strain $\overline{\varepsilon}_0$, which has an influence on the creep at the calculation point $t_i$, the other effects are all zero. For a long-span concrete continuous-girder bridge constructed by segmentation, the creep will generate secondary internal forces that will cause changes in the elastic stress and strain at each calculation time point. The creep effect is cumulative; therefore, it is necessary to consider the effect of the elastic strain increment of each calculation point on the subsequent calculation point. The batch mode of ANSYS can be revoked by the programming languages, e.g., C++ and MATLAB [20]. In this study, the FE results are read by MATLAB, and the initial strain input data of the subsequent calculation time points are calculated and generated. The FE calculation and the stress redistribution are completed by ANSYS in the batch mode. The flow chart is shown in Figure 1. In the computation of a time point, i.e., time $t_i$, we first read the increase in strain of the preceding steps and recall the relevant creep coefficient. We then obtain the initial data of the current step: $\overline{\varepsilon}_0 \cdot \phi(t_i, t_0) + (\overline{\varepsilon}_1 - \overline{\varepsilon}_0) \cdot \phi(t_i, t_1) + \cdots + (\overline{\varepsilon}_{i-1} - \overline{\varepsilon}_{i-2}) \cdot \phi(t_i, t_{i-1})$. ANSYS is then revoked to complete the FE analysis and to output the result of the current step. This loop will be controlled by MATLAB and will continue till attaining the objective computation time point and completing the analysis.

*2.2. Shear Creep Coefficient.* Specifications and research institutions have different creep functions, but they can basically be expressed as the product of the creeping ultimate value and the development function. For example, according to JTG 3362-2018 [19], the creep function formula is as follows:

$$\phi(t, t_0) = \phi_0 \cdot \beta_c(t - t_0), \tag{3}$$

where $\phi_0$ is the final value (nominal creep coefficient), related to the concrete grade, loading age, component thickness, and environmental humidity. $\beta_c(t - t_0)$ is a creep development function, used to calculate the creep deformation at a certain time $t$, divided into exponential

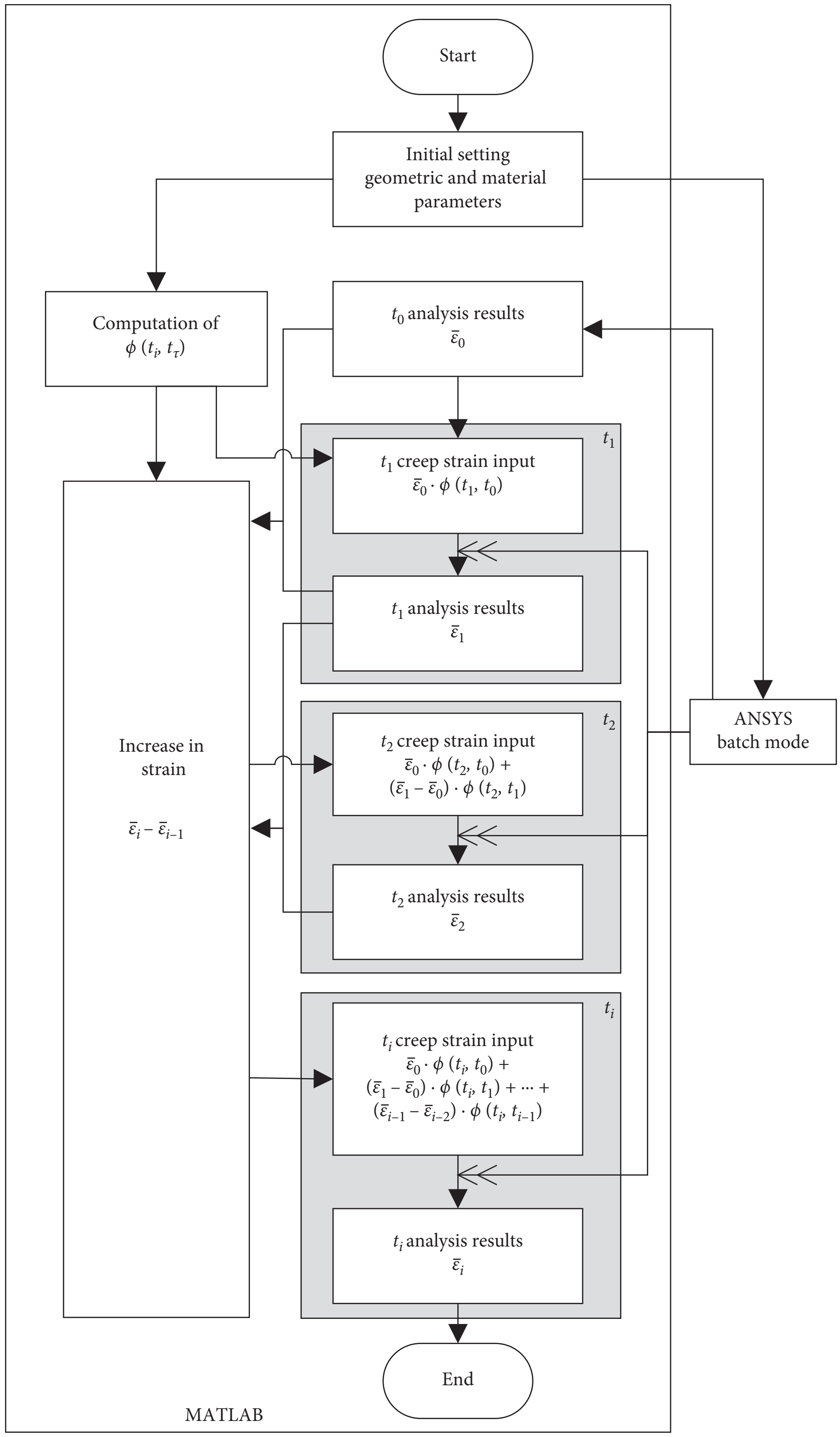


Figure 1: Flow chart of creep calculation.

functions, as well as the form of the score and the sum. In this study, $\beta_c(t - t_0) = [((t - t_0)/t_1)/(\beta_H + (t - t_0)/t_1)]^{0.3}$, where $t$ is the targeted computation time, $t_0$is the concrete age when loading is applied, $\beta_H = 150[1 + (1.2(\mathrm{RH}/\mathrm{RH}_0))^{18}](h/h_0) + 250 \leq 1500$, RH is the yearly average humidity, $h$ is the nominal depth in units of mm and equal to $2A/u$, $A$ is the area of the girder section, and $u$ is the length of the edge exposed to the atmosphere. The current creep coefficient of concrete is tested by axial loading. The creep coefficient in the shear direction has rarely been reported. A recent experimental study showed that the one-year shear creep of three torsion columns made of C30 concrete may attain twice the creep of the axial member [21]. However, further long-term laboratory and field tests of high-grade concrete are needed for general application purposes. In this study, based on the normative formula as shown in Equation (3) and considering the concrete grade of the prototype bridge, the creep correction coefficient $m\_\phi$ for shear creep consideration is used within a fluctuation range of 50% (0.5, 1.0, and 1.5) to analyze the influence of the shear creep coefficient on the long-term deflection of the bridge.

Another ingredient of time-dependent deformation in equation (1) is shrinkage that is independent of the stress state so that the expression of the shrinkage strain can be written directly [19]: $\varepsilon_{cs}(t, t_s) = \varepsilon_{cso} \cdot \beta_s(t - t_s)$, where $\varepsilon_{cso}$ is the ultimate shrinkage value and $t_s$ is the age of the concrete at the beginning of shrinkage related to the curing date and is different from the value of $t_0$ used in developing the creep function. In addition, the function $\beta_s$ is developed in a like manner to that of creep: $\beta_s(t - t_s) = [((t - t_s)/t_1)/350(h/h_0)^2 + (t - t_s)/t_1]^{0.5}$.

*2.3. Consideration of Segmental Construction.* For bridges using the falsework construction method, the age of each part of the structure is the same. Taking the calculation time $t_0$ as an example (assuming the concrete age is $t_0$), the creep function of all the concrete for the subsequent calculation moments $t_0$ is the same, namely, $\phi(t_i, t_0)$. In contrast, for bridges with the segmental construction method, the concrete age of each section is different. Correspondingly, the creep function is different for the subsequent calculation time $t_i$. For example, if the age of section A is $t_0$ and section B is poured $\Delta t$ days later than A, the age of section B should be $t_0 + \Delta t$. Therefore, the creep coefficients of the two segments at the calculation moment $t_i$ are $\phi(t_i, t_0)$ and $\phi(t_i, t_0 + \Delta t)$ for sections A and B, respectively. Additionally, concrete of multiple ages is commonly seen in long-span concrete girder bridges constructed using the cantilever construction method. In such cases, the age difference between the first and the last pouring sections can reach hundreds of days; subsequently, the creep coefficient varies greatly. Therefore, the difference in age should be considered. In the ANSYS modeling process, the elements are grouped according to the construction section. When MATLAB recalls the creep coefficient module, the element group is first identified and the corresponding loading age is then given. Finally, the initial strain input data of the subsequent calculation time can be generated.

## 3. Calculation of the Prototype Bridge

*3.1. Structural Parameters.* To illustrate the effect of shear creep on long-term deflection, a prestressed concrete continuous girder bridge with a main span of 100 m is used as background. This bridge is located on a highway in Guangdong, China. It is a prestressed concrete continuous girder bridge with a span combination of 65 + 100 + 65 m (Figure 2(a)). The traffic lanes are dual direction and are separated on two independent bridges with a gap of 1.274 m. The single-room box section was used in the superstructure layout. The depth of the girder section over the pier is 5.6 m, decreasing to 2.2 m at the midspan section. The bottom of the box girder varies from the midspan to the top of the pier according to the formula for a parabola. The width of the box girder is 11.898 m, with a 1.5 m pedestrian way connected to the flange, as shown in Figure 2(b).

The main beam used C50 concrete. The girder section over the pier is arranged with prestress tendons in the flange and the web, each consisting of 26 tendons. The prestressed midsection contains 20 tendons in the bottom slab. Each tendon consists of twelve 15.2 mm diameter high-strength and low-relaxation steel strands. The vertical prestressing consists of a 25 mm diameter fine-rolled rebar, and the spacing is 60 cm around the sections over the piers and 65 cm at other locations. We use a simplified manner to consider initial prestress loss of the tendons, in which the "effective prestress" of 1350 MPa on longitudinal tendons and 675 MPa on vertical tendons are used. The long-term prestress loss caused by creep and shrinkage deformation will be automatically considered by the program.

The cantilever segmental casting process is divided into 16 segments (blocks #0~#15), of which block #15 is the closure segment. The side spanning cast-in segment consists of blocks #16~#18. The lengths of the segments are 2 m~4 m. Each segmental construction step lasts approximately 7 days. The concrete ages of the closure segment and the pier #0 block are different by 105 days. When calculating the creep during the operation of the bridge, the creep coefficient of the corresponding age is adopted for each segment. Material parameters are listed in Table 1.

The prototype bridge was completed and opened to traffic in the 1990s. A significant downward deflection in the midspan was observed in 2001. A full-bridge deformation observation system was then established. The observation points were placed along the central reservation and the safety barriers at both sides. In all, 34 measuring points were distributed over each side of the bridge. Their locations are shown in Figure 3(a). During the following 10-year period, the midspan of the bridge continued to deflect. As shown in Figure 3(b), the maximum relative deformation of the left span is 16 cm and that of the right bridge is 21 cm, which are close to or larger than the specification deformation limit 1/600 of the span length. This made a difference in the appearance of the bridge (Figure 3(b)) and affected driving comfort. The side span had a certain camber, with a maximum value of approximately 10 cm.

*3.2. FE Model Parameters.* The background bridge model is established by ANSYS. To consider the shear deformation, the concrete box beam adopts the element SHELL181, including in-plane and out-of-plane bending stiffness (KEYOPT (1) = 0). The exact integral calculation (KEYOPT (3) = 2) is adopted. The prestressed tendons are simulated by the element LINK180, and the prestress forces are applied by

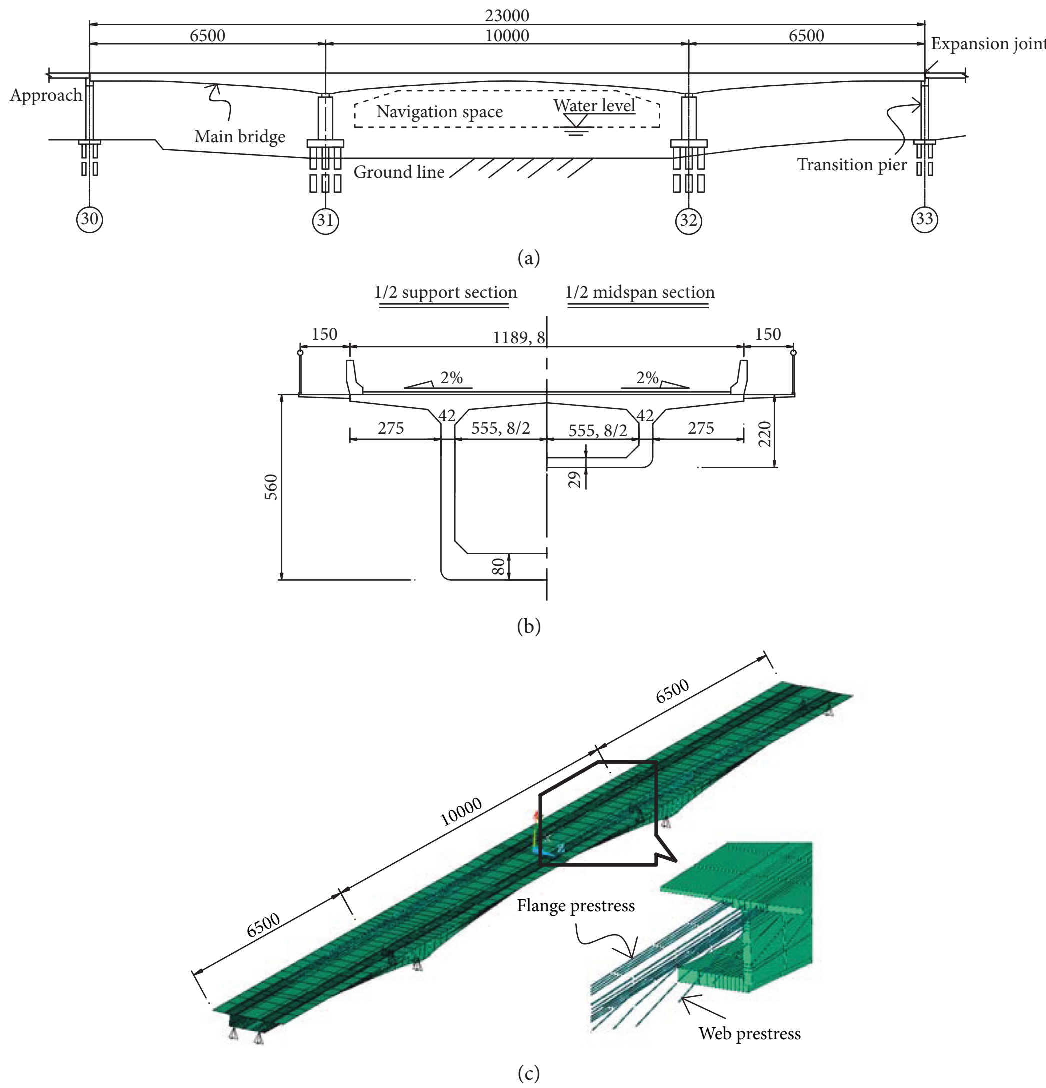


Figure 2: Model of the prototype bridge (unit: cm). (a) Elevation. (b) Cross section of box girder. (c) ANSYS model and prestress.

Table 1: Parameters of modeling.

| Term | Value |
|---|---|
| Grade of concrete | C50 |
| Average humidity (RH) | 70% |
| $t_0$ (d) | 5 |
| $t_s$ (d) | 3 |
| Time interval between adjacent segments (d) | 7 |
| Initial prestress of longitudinal tendon (MPa) | 1350 |
| Initial prestress of vertical tendon (MPa) | 675 |

decreasing the equivalent temperature. The FE model is shown in Figure 2(c), and the materials used are shown in Table 1.

The long-term deformation of concrete girder bridges is caused by the long-term effect of dead load and the camber by prestress. As the creep of concrete under dead load affects the prestress loss, they are therefore interrelated and can be automatically included in the spatial model. In addition, live load also has a certain impact on bridge deflection, but the proportion is usually low. After vehicles leave the bridge, the bridge deck alignment is restored. While the cumulative effect of residual deformation under live load and its impact on concrete fatigue does need to be studied, in this paper the effect of live load is ignored, and only the long-term deformation under dead load is considered.

## 4. Results and Discussion

*4.1. Effect of Shear Creep.* The deformation of girder bridges is mainly due to the bending moment of the dead load, which grows significantly with increasing design span length. It becomes difficult to set the prestressing steel tendons in the limited section space of long-span girder bridges to completely compensate for the dead-load moment. As shown in Table 2, the prestress bending moment is less than dead load bending moment at the section over pier of the 100 m span bridge, which results in the overall deflection of the bridge. At the same time, the bending moment distribution of a 270 m main span bridge [1] is calculated.

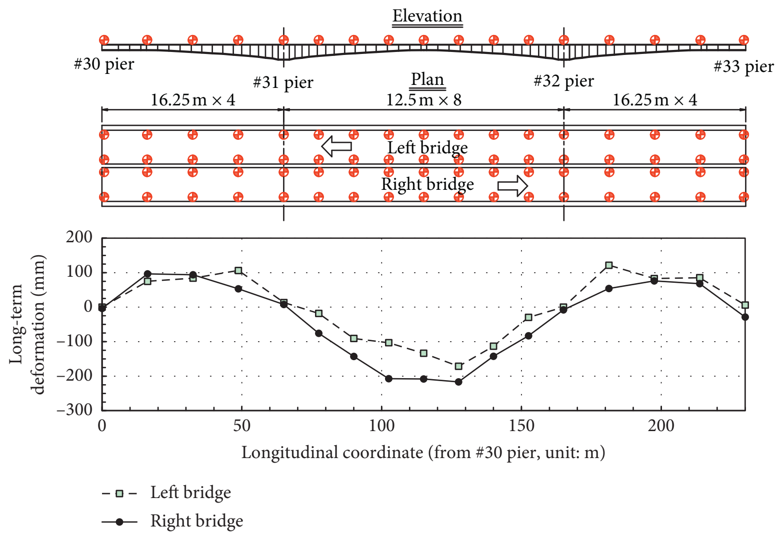


(a)

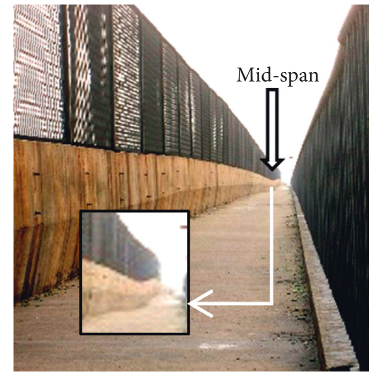


(b)

Figure 3: Deformation investigation of the prototype bridge. (a) Investigation points of the deck and long-term deformation over 10 years. (b) Deflection of midspan (pedestrian parapet view).

Table 2: Comparison of bending moments of the critical section (unit: kN·m).

| Bridge span length | Section over pier | | | Midspan section | | |
|---|---|---|---|---|---|---|
| | Dead load (1) | Prestress (2) | (2)/(1) | Dead load (1) | Prestress (2) | (2)/(1) |
| 100 m | $-2.75E+05$ | $2.54E+05$ | $-0.92$ | $5.68E+04$ | $-6.80E+04$ | $-1.20$ |
| 270 m | $-2.30E+06$ | $1.99E+06$ | $-0.86$ | $2.78E+05$ | $-2.02E+05$ | $-0.73$ |

The ratios of the prestress bending moment to the dead-load bending moment at pier top and midspan are 0.86 and 0.73, respectively. The trend of bridge deflection becomes obvious with increasing span.

As shown in Figure 4(a), the main span of the prototype bridge deflected, and the side span cambered under dead load. The deflection will be further developed according to the elastic deformation of dead load due to the inherent creep characteristics of concrete. Ten years after the completion of the bridge, the total deformation of the main span will reach 2.57 times of the elastic deflection. As shown in Figures 4(b) and 4(c), for elastic deformation and long-term deformation, the calculated values considering shear deformation are larger than those without considering shear deformation. When the bridge is completed, the midspan deflection considering shear deformation is 6.9 cm, and the midspan deflection excluding shear deformation is 6.1 cm. Without considering shear deformation, the elastic deformation will be reduced by 12.5%. After 10 years of operation, the calculated value considering shear deformation is 17.7 cm and the calculated value excluding shear deformation is 15.8 cm.

In the practical construction of bridges, the elastic deformation can be eliminated by setting the precamber and adjusting the elevation of the vertical formwork of each segment in the construction process so that the alignment of the completed bridge can meet the design requirements. Therefore, the long-term relative deformation that affects the performance of bridges is based on the alignment of completed bridges. For the research prototype bridge, as shown in Figure 4(d), the calculated value of relative deformation considering shear is 12.4% larger than that of nonshear relative deformation. The error of the shear effect in calculating long-term deformation should not be ignored.

*4.2. Effect of Creep Coefficient.* As a mixed material, concrete is highly discrete and stochastic, in which the mechanical properties are different in different locations of bridges even in the same batch of concrete. The creep coefficient is the main parameter used to characterize the creep characteristics of concrete. Gilbert points out that the creep deviation of concrete can reach more than 50% [18]. There are few studies at present on the shear creep coefficient. Bažant et al. took the 3D creep into account using the method of creep rate, assuming that the shear creep coefficient is the same as that in the axial direction [11]. In this paper, the influence of shear creep and axial creep on the overall linear deformation of bridges is calculated using the creep correction coefficients $m_{xy}, m_{yz}, m_{xz}$. In this study, we consider shear creep by using three series of coefficients: 0.5, 1.0, and 1.5 times the standard axial creep coefficient. The factor of 1.0 times the standard axial creep coefficient means the shear creep coefficient is identical to the standard axial creep coefficient. Likewise, the factors of 0.5 and 1.5 indicate that the shear creep coefficient the computation used is 50% smaller or larger compared with the standard axial creep coefficient. The analysis is divided into three cases based on

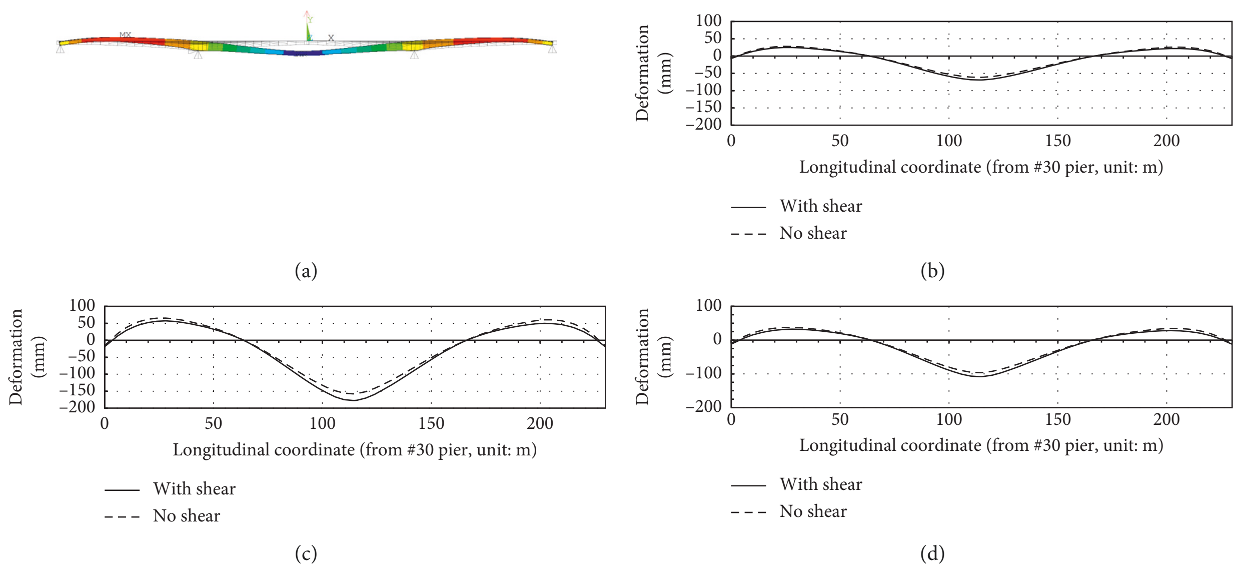


Figure 4: Long-term deformation of the prototype bridge. (b) Age: 0 days. (c) Age: 3650 days, absolute value. (d) Age: 3650 days, relative value c–b.

the value setting of the creep correction coefficients $m_{xy}$, $m_{yz}$, $m_{xz}$: (1) 0.5; (2) 1.0, and (3) 1.5.

As shown in Figure 5, the midspan deflection develops rapidly within 5 years (1825 days) after completion of the bridge and more than 90% of the ultimate creep deformation takes place. For example, in the case of 1.0 shear, the midspan displacement is 104.4 mm at 5 years and sags only slightly more to 110.6 mm at 20 years. When the shear creep coefficient increases, the trend of the bridge deformation remains the same, but the deflection value increases. The long-term deflection has a linear relationship with the shear creep coefficient (Figure 5(a)). For example, in the analysis of the midspan long-term deformation of 20 years, the midspan deflection increases from 110.5 mm to 116.4 mm (by approximately 5%) with the shear creep coefficient increasing from 1.0 to 1.5.

*4.3. Effect of Different Degrees of Prestress.* The long-term deflection of the bridge consists of two parts: the prestressing camber and the dead load deflection, both of which contain shear creep components. To analyze the shear and creep effects on bridges with different degrees of prestress, the stress of the prestress tendon is taken as a parameter for analysis.

As shown in Figure 6, the change in the degree of prestress has an obvious influence on the elastic deflection and long-term deflection of the middle span. For every 10% reduction in the degree of prestress, the initial elastic deflection and long-term deflection increase by approximately 10%. The results show that the effect of shear creep remains stable even when the degree of prestress is different. In the calculation of long-term deformation of the bridge, the displacement accounted for by the shear creep is 10.5–12.5% larger than that without considering the shear effect. It can be seen that, for the same bridge, a unified amplification factor can be used to consider the effect of shear creep when the degree of prestress is different.

To further illustrate the influence range of shear deformation, a continuous rigid-frame bridge model with a 270 m main span is established. The height of the section over a pier is 14.17 m, and the midspan section is 3.2 m high. The detailed structural parameters of the bridge can be found in the relevant literature [1]. The long-term deformation at 20 years is calculated as shown in Figure 7. The long-term deformation value increases by approximately 14.6% considering shear creep. In conclusion, combined with the analysis of 100 m and 270 m main span concrete continuous girder bridges, the long-term deformation deflection calculated by the planar frame system program can be multiplied by the magnification factor of 1.13–1.15 to consider the effect of shear creep.

There are corresponding specifications and suggestions for the calculation of long-term deformation of concrete structures in specification and codes, including the limit value and calculation method. In terms of the limit value, CEB-FIP [22] ensures stiffness by limiting span-to-height ratio, while Chinese codes adopt the method of limiting the final value of long-term deformation, which is consistent with AASHTO [23]. The creep formula of the JTG 3362-2018 code [19] is similar as CEB-FIP. In addition, a simplified method for calculating the final value of long-term deformation is provided, in which the short-term elastic deflection is multiplied by the long-term growth factor $\eta_\theta$, and the obtained value is related to the strength of concrete. According to the above analysis, if the elastic deflection is calculated by the planar frame system program, the long-term deflection magnification factor affected by shear creep should be considered.

*4.4. Effect of Vertical Prestress.* Because a box section is often used in long-span concrete girder bridges, the spatial stress characteristics are remarkable. In addition to longitudinal prestressing tendons, transverse prestress of the flange and

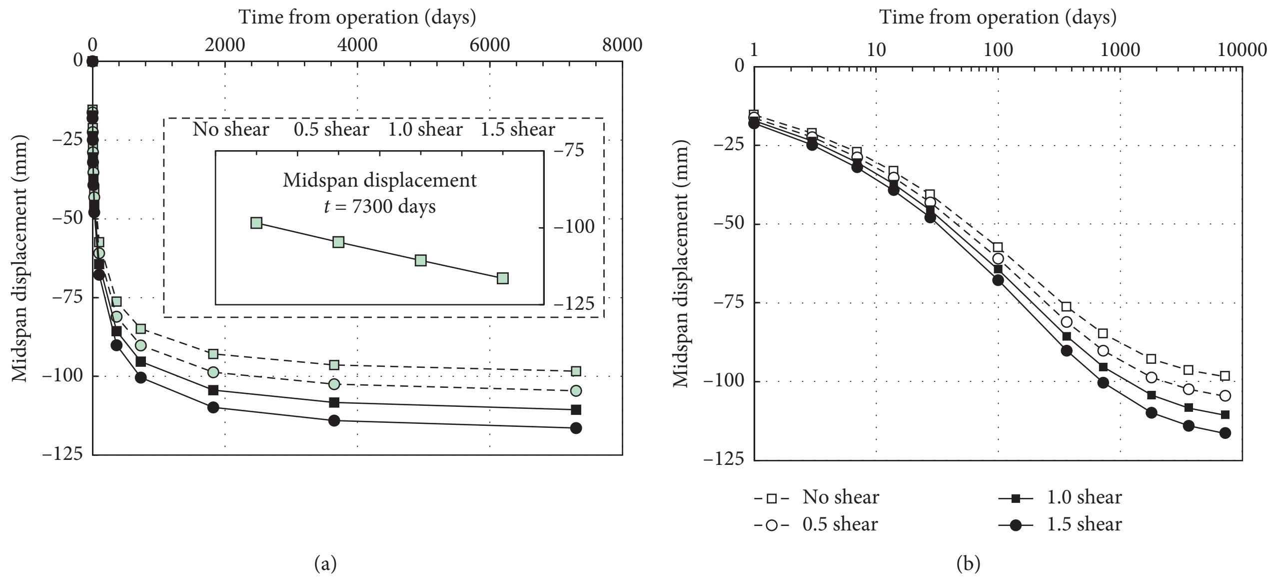


FIGURE 5: Deflection of midspan with different shear creep coefficients. (a) Linear coordinates. (b) Logarithmic coordinates.

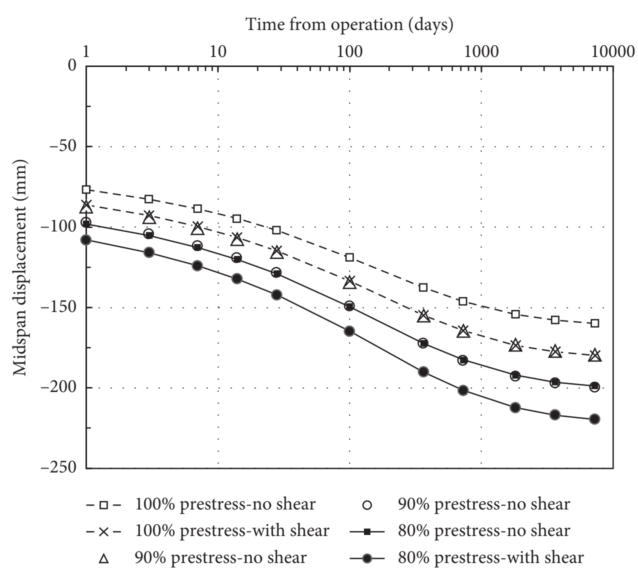


FIGURE 6: Deflection of midspan with different degrees of prestress.

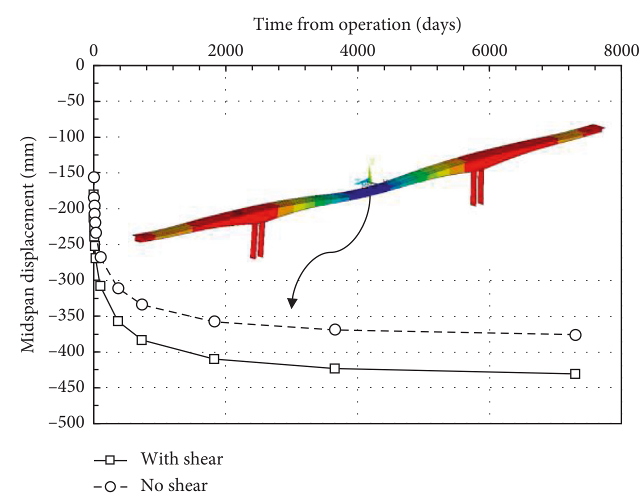


FIGURE 7: Long-term midspan deflection of a continuous rigid bridge with a main span of 270 m.

vertical prestress of webs are also set up to form a three-dimensional prestressing system. Vertical prestressing can improve the shear capacity of the cross section. In some bridge designs, the downward bending of webs is cancelled for the convenience of construction so that the shear capacity is completely provided by the concrete and vertical prestressing. For service performance, the role the vertical prestressing can play in long-term deformation is studied. We compare two cases: (1) setting up vertical prestressing tendons using tensioning and (2) setting up vertical prestressing tendons without tensioning. The results show that, even considering shear creep, the application of vertical prestressing has no effect on the long-term deflection (the calculation results are consistent with the previous results, so they are not listed). The reason is that according to the equivalent load method, the vertical prestressing force is equivalent to two vertical concentrating forces on the top along the box girder section, which has no effect on the shear force on the structure and has little effect on the stiffness of the structure, so it cannot reduce the long-term deformation of the structure. It can be seen that the increase in vertical prestressing force can only increase the shear capacity of the superstructure but cannot reduce the long-term deformation. In addition, the long-term loss of prestressing near the top of the middle pier is relatively large, the loss at which in 20 years is approximately 3.7%, whereas at other locations, it is less than 1%, as shown in Figure 8.

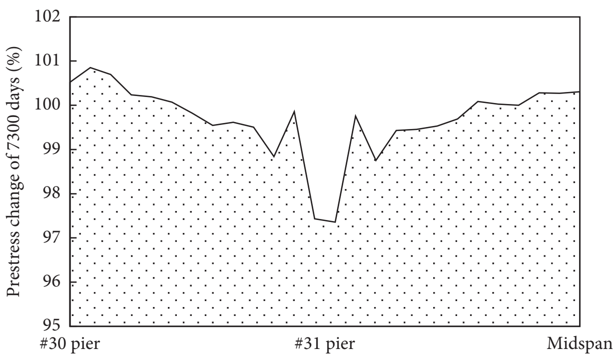


Figure 8: Prestress loss distribution of vertical prestress (half structure).

## 5. Conclusions

How to accurately predict the long-term deformation and mechanical characteristics of long-span concrete girder bridges is of great importance. In this paper, the conclusions on the influence of the studied shear creep are as follows:

(1) A three-dimensional creep calculation program based on the superposition principle is developed by MATLAB and ANSYS, which provides a separate interface for the shear creep coefficient. The analysis of the prototype bridge shows that the long-term deformation increases by 12.5% after shear creep is considered. It is suggested that the long-term deformation be calculated by multiplying the magnification factor of shear creep of 1.13–1.15 based on the analysis results of the general planar frame program.

(2) The parameter analysis of the shear creep coefficient shows that the long-term deformation of long-span concrete girder bridges is proportional to the shear creep coefficient. The shear creep effects of bridges with different degrees of prestress are close, so a unified amplification factor can be adopted.

(3) Vertical prestressing has no effect on the shear creep and long-term deformation of bridges. The long-term loss of vertical prestressing with time is relatively large at the pier top section.

(4) The three-dimensional creep calculation method in this paper considers the age variation in concrete and the influence of the shear creep coefficient, which can provide a reference for the fine analysis of creep of concrete bridges.

The long-term deflection of long-span concrete girder bridges is a complicated engineering problem involving materials, design, construction, maintenance, and management. Attention is confined herein to the calculation error with the limitation of the linear elastic stage of materials. It has been found that the deflection of concrete bridges is accompanied by cracks, which indicates that the stress of concrete is approaching or exceeding the ultimate strength. In such case, it will be unsafe to use the assumption of linear creep. There is an urgent need for accurate consideration of the effect of nonlinear creep on the behavior of long-term deformation in subsequent research.

## Data Availability

The measured data included in the article are freely available.

## Conflicts of Interest

The authors declare no conflicts of interest.

## Acknowledgments

This study was supported by the National Science Foundation of the People's Republic of China (51208056) and the Fundamental Research Funds for the Central Universities (310821161013 and 300102218213).

## References

[1] Z. P. Yang, G. X. Zhu, and W. Li, "Long-term deflection investigation of prestress concrete rigid bridge," *Highway*, vol. 49, no. 8, pp. 285–289, 2004.

[2] Z. H. Lou, "Main faults in large span beam bridges," *Journal of Highway and Transportation Research and Development*, vol. 23, no. 4, pp. 84–87, 2006.

[3] Y. W. Niu, X. F. Shi, and X. Ruan, "Measured sustained deflection analysis of long-span prestressed concrete beam bridges," *Engineering Mechanics*, vol. 25, no. S1, pp. 116–119, 2008.

[4] I. N. Robertson, "Prediction of vertical deflections for a long-span prestressed concrete bridge structure," *Engineering Structures*, vol. 27, no. 12, pp. 1820–1827, 2005.

[5] J. Xie, G. L. Wang, and X. H. Zheng, "Review of study of long-term deflection for long span prestressed concrete box-girder bridge," *Journal of Highway and Transportation Research and Development (English Edition)*, vol. 2, no. 2, pp. 47–51, 2007.

[6] X. Q. Meng, L. F. Wei, J. C. Zhang et al., "Study of down warping in the midspan of long-span rigid frame bridge," *World Bridges*, vol. 41, no. 2, pp. 76–79, 2013.

[7] F. W. Wang and X. F. Shi, "Study on long-term deflection control of large span prestressed concrete girder bridge," *Shanghai Highways*, vol. 25, no. 1, pp. 29–32, 2006.

[8] H. J. Li, J. Liu, R. X. Wang et al., "Effect of segmental joints on structural deformation in long-span prestressed concrete box girders," *Journal of Basic Science and Engineering*, vol. 21, no. 3, pp. 562–568, 2013.

[9] J. Wang, J. C. Zhao, and L. X. Liu, "Numerical relationship between creep coefficient and creep deflection coefficient of prestressed concrete beams effected by partial pre-stressing ratios," *Journal of Zhengzhou University (Engineering Science)*, vol. 34, no. 5, pp. 26–30, 2013.

[10] J. Q. Bu and J. C. Cui, "Impacts of prestress loss on the deflection for large-span prestressed concrete continuous girder bridges," *Journal of Railway Engineering Society*, vol. 31, no. 7, pp. 57–61, 2014.

[11] Z. P. Bažant, Q. Yu, and G.-H. Li, "Excessive long-time deflections of prestressed box girders. II: numerical analysis and lessons learned," *Journal of Structural Engineering*, vol. 138, no. 6, pp. 687–696, 2012.

[12] G. H. Cao, S. Zhang, W. Zhang, and X. R. Peng, "Long-term deflection test and theoretical analysis on cracked prestressed

concrete box beams," *KSCE Journal of Civil Engineering*, vol. 22, no. 2, pp. 688–695, 2018.

[13] T. Guo and Z. Chen, "Deflection control of long-span PSC box-girder bridge based on field monitoring and probabilistic FEA," *Journal of Performance of Constructed Facilities*, vol. 30, no. 6, pp. 4016053–4016110, 2016.

[14] Y. W. Niu, X. F. Shi, and X. Ruan, "A Finite element analysis method of concrete structure with three dimensional creep," *Journal of Tongji University (Natural Science)*, vol. 37, no. 4, pp. 475–480, 2009.

[15] H. D. Huang, Z. F. Xiang, and J. L. Zheng, "Refined analysis of three-dimensional creep effect for PC box-girder bridges," *Journal of China Highway*, vol. 26, no. 5, pp. 108–114, 2013.

[16] Z. T. Lv and Z. F. Pan, "Issues in design of long-span prestressed concrete box girder bridges," *China Civil Engineering Journal*, vol. 43, no. 1, pp. 70–96, 2010.

[17] W. X. Zhang, Z. T. Tan, and K. Xue, "Analysis of shrinkage and creep of reinforced concrete based on ABAQUS," *Journal of Xi'an University of Architecture & Technology (Natural Science Edition)*, vol. 47, no. 3, pp. 347–353, 2015.

[18] R. I. Gilbert, *Time Effects in Concrete Structures*, Spon Press, Newyork, NY, USA, 2011.

[19] CCCC Highway Consultants Co., Ltd, *Code of Design of Highway Reinforced Concrete and Prestressed Concrete Bridges and Culverts JTG 3362-2018*, China Communications Press, Beijing, China, 2018.

[20] M. Pouraminia and M. Ghaemian, "Shape optimization of concrete open spandrel arch bridges," *Građevinar*, vol. 67, no. 12, pp. 1177–1185, 2015.

[21] Y. W. Niu, H. E. Cao, Y. Y. Tang, and T. Wang, "Concrete torsion shear creep experimental method and application," *Journal of Tongji University (Natural Science)*, vol. 47, no. 7, pp. 475–480, 2019.

[22] CEB-FIP, *Model Code 1990 (Design Code)*, Thomas Telford Press, Lausanne, Switzerland, 1993.

[23] American Association of State Highway and Transportation Officials, *LFRD Bridge Design Specifications*, American Association of State Highway and Transportation Officials, Washington, DC, USA, 8th edition, 2017.